RSC Sustainability

ROYAL SOCIETY OF CHEMISTRY

PAPER

View Article Online
View Journal | View Issue

Cite this: *RSC Sustainability*, 2025, **3**, 395

Synthesis of *N*-formamides *via* oxidative carbonylation of amines with paraformaldehyde over a CoNC catalyst†

Longfei Wang,‡[a] Yuanyuan Hu,‡[ab] Qingqing Pu,[a] Yongqiang Yao,[a] Hao Zhang,[a] Yong Guo,[a] Yongsheng Li,*[a] Bin Dai[a] and Zhengang Ke*[a]

Received 23rd September 2024
Accepted 11th November 2024

DOI: 10.1039/d4su00591k

rsc.li/rscsus

N-Formamides are important high-value chemicals with a wide array of applications. Whilst the oxidative carbonylation of amines with paraformaldehyde is a green route to synthesize *N*-formamides, the reaction suffers from the drawback of having to use noble metal catalysts. Herein, a non-noble metal CoNC catalyst was developed for the oxidative carbonylation of amines with paraformaldehyde. A series of N-heterocycles, aliphatic amines and anilines with different substituents were suitable for reaction over this CoNC catalyst, and moderate to good yields of the *N*-formylated amines were obtained. A mechanistic investigation suggests that both singlet oxygen ($^1O_2$) and the superoxide anion (O_2^-) are the active oxygen species of the oxidative carbonylation reaction. Co-N_x single atom sites are the possible catalytic active sites on the CoNC catalyst.

Sustainability spotlight

N-Formamides are important high-valuable chemicals with a wide array of applications. Whilst the oxidative carbonylation of amines with paraformaldehyde is a green and sustainability route to synthesize *N*-formamides, the reaction suffers the drawback of having to use noble metal catalysts. Catalysis using abundant metals is more in line with the concept of green sustainable development. Herein, a non-noble metal CoNC catalyst was developed for the oxidative carbonylation of amines with paraformaldehyde.

Introduction

Carbonylation is a general method to produce chemicals containing carbonyl groups, such as aldehydes, alcohols, and amides.[1–3] The hydroformylation of olefins with CO and hydrogen stands out as one of the most important chemical industrial processes, with an annual production capacity of nearly 24 million metric tons.[4–8] Alternatively, the carbonylation of amines is another important route to synthesize amides.[9–12] *N*-Formamides are specific amides with a hydrogen atom connected with the carbonyl carbon atom, which are widely used in organic synthesis and biological pharmaceutical intermediates, particularly in small drug molecules, peptides and nucleic acids.[13–15]

N-Formamides are synthesized *via* the reaction of amines with carbonyl reagents such as CO, triethyl orthoformate, chloral, glyoxylic acid, and ethyl acetate. This reaction suffers from drawbacks such as toxic raw materials and low atom-economy.[16–18] In recent years, a series of green *N*-formylation routes were developed,[19–21] for example, the oxidative carbonylation of amines with methanol[22–24] or formaldehyde,[25–30] the dehydration condensation of amines with formic acid,[14,31] and the reductive carbonylation of amines with CO_2/H_2 (ref. 32–37) (Scheme 1). The oxidative carbonylation of amines with formaldehyde is a fascinating route for the synthesis of *N*-formamides because the starting materials are widely available and water is the only by-product, and thus it can be performed under mild conditions which is favorable for the synthesis of drug molecules.[38]

Formaldehyde is conveniently obtained *via* the aerobic oxidation of renewable methanol[39–41] over a silver catalyst.[42,43] Since a pioneering work on the oxidative carbonylation of amines with formaldehyde over an iridium complex,[26] a series of Au/PVP,[25] Ag (110),[27] Au/CNT,[28] Au/Al_2O_3 (ref. 29) and Au/TiO_2 (ref. 30) catalysts were developed for the reaction (Scheme 1 and Table S1, ESI†). Although the above catalysts are effective for the oxidative carbonylation of amines with formaldehyde, they suffer from the drawback of having to use noble metal catalysts which hamper their industrial applications.[44] It is therefore

[a]*School of Chemistry and Chemical Engineering, State Key Laboratory Incubation Base for Green Processing of Chemical Engineering, Shihezi University, Shihezi, 832003, China. E-mail: ysli@ecust.edu.cn; zgke@shzu.edu.cn*

[b]*First Affiliated Hospital of Shihezi University, Shihezi, 832008, China*

† Electronic supplementary information (ESI) available. See DOI: https://doi.org/10.1039/d4su00591k

‡ These authors contributed equally to this work.

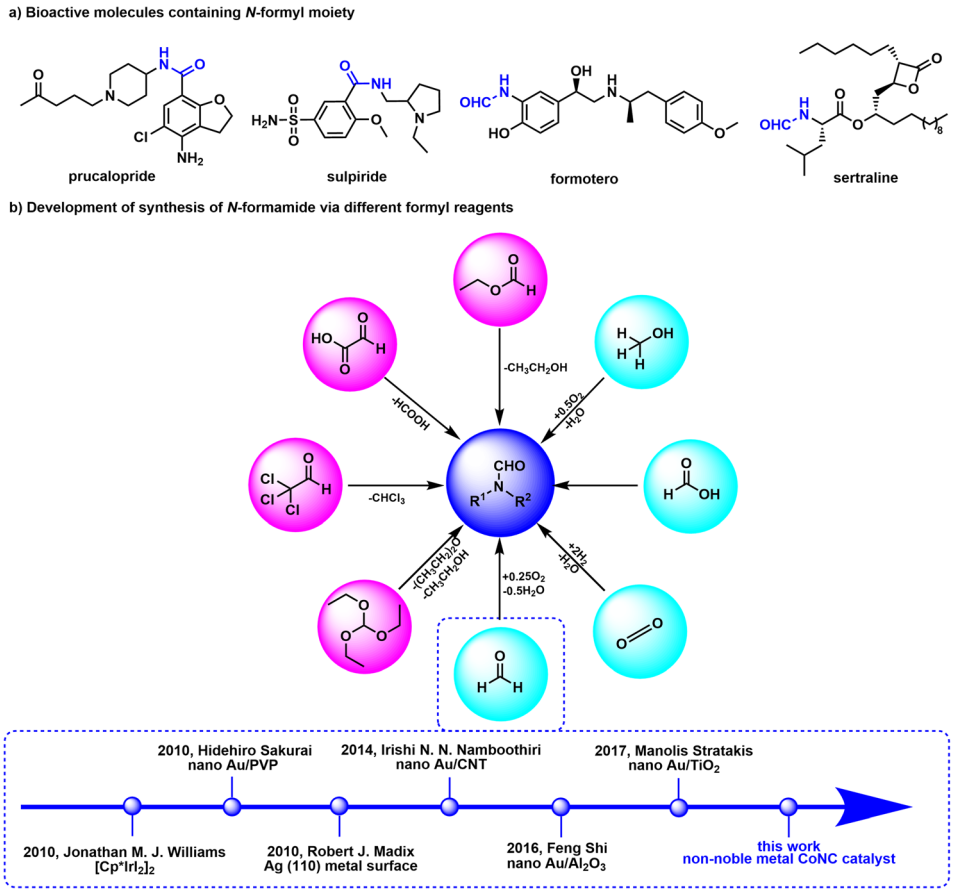

Scheme 1 Overview of the oxidative carbonylation of amines with paraformaldehyde.

imperative to develop non-noble metal catalysts for the oxidative carbonylation of amines with formaldehyde.[19]

Nitrogen-doped carbon supported metal (MNC) catalysts are considered to be a substitute for Pt-based catalysts in electrochemical oxygen reduction reactions.[45–48] Because of its unique cation metal center and metal nitrogen coordination structure, MNC have attracted increasing interest for use in thermocatalytic reactions. For example, the oxidation of alcohols to carboxylic acids,[49,50] the oxidative esterification of alcohols to esters,[49,51] the ammoxidation of alcohols to nitriles or amides,[49,50] and the oxidative dehydrogenation of N-heterocycles.[52–54] However, the oxidative *N*-formylation of amines with formaldehyde over MNC catalysts remains undeveloped. Cobalt has a specific electronic structure, and it has been established as one of the most important non-noble metal catalysts in hydrogen transfer[55] and aerobic oxidation reactions.[50,56–59]

Herein, a non-noble metal CoNC catalyst was developed *via* pyrolysis of the complex formed between a cobalt salt (*e.g.*, $CoCl_2$) and ligand (*e.g.*, phenanthroline). The resulting catalyst allows for the oxidative carbonylation of N-heterocycles, aliphatic amines, and aromatic amines with paraformaldehyde under mild conditions. Free radical quenching experiments show that both singlet oxygen ($^1O_2$) and the superoxide anion (O_2^-) are the possible active oxygen species during the reaction with this CoNC catalyst.

Results and discussion

To evaluate the catalytic performance of the synthesized MNC material, morpholine (**1a**) was selected as the model substrate to investigate the oxidative carbonylation reaction of an amine with paraformaldehyde (Fig. 1). **1a** was found to be unreacted over the NC-700 catalyst, which suggests that the nitrogen-doped carbon support did not activate the reaction. Of all the prepared MNC catalysts tested, the reaction hardly proceeded over NiNC-700, CuNC-700 and ZnNC-700, indicating that Ni, Cu, and Zn were not the active metals for the reaction. 8% of *N*-formylmorpholine (**1b**) was obtained over MnNC-700, and a 31% yield of **1b** was obtained over the FeNC-700 catalyst. The yield of **1b** reached up to 90% over CoNC-700, suggesting that Co was the most active metal for the reaction (Fig. 1a). To explore the reaction selectivity, GC-MS was performed to detect the possible by-products of the reaction when it was conducted at 30 °C. Aside from the peaks for product **1b** and the standard dodecane, three new peaks at 3.458, 6.026, and 10.501 min were detected (Fig. S1 and ESI†), belonging to *N*-methyl morpholine, 4-(methoxymethyl)morpholine and *N*,*N*′-dimorpholinomethane, respectively. According to our previous report, *N*,*N*′-

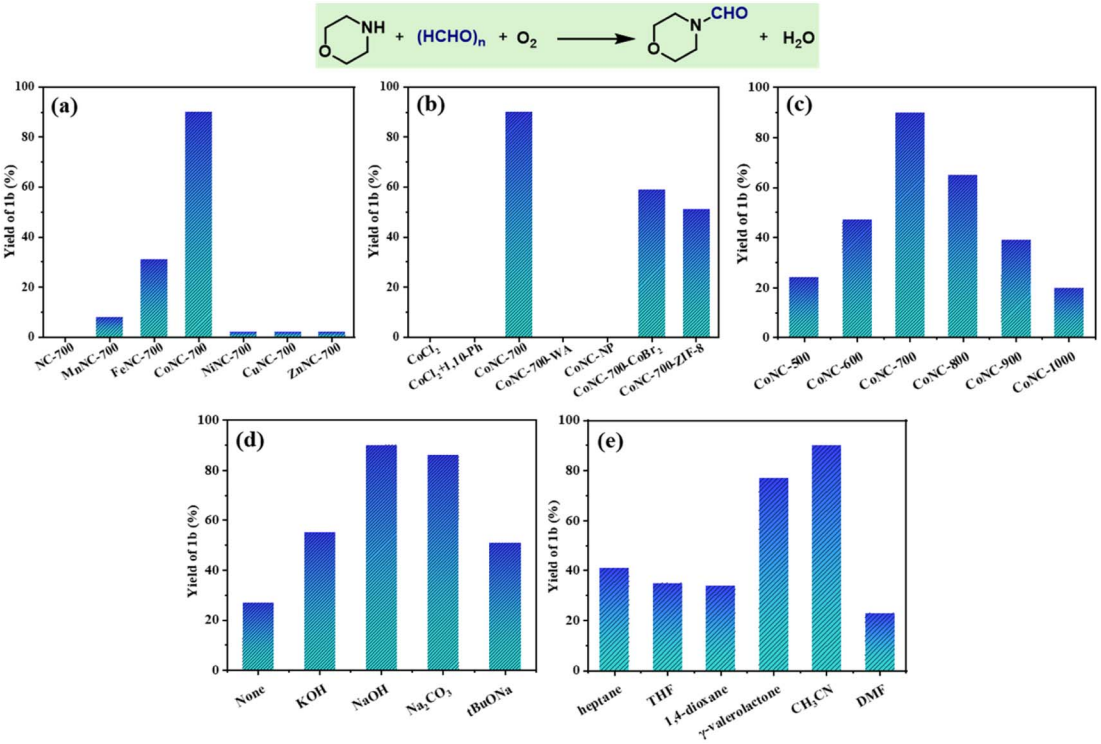

Fig. 1 (a) and (b) Oxidative carbonylation of morpholine with paraformaldehyde over different catalysts and (c) over CoNC catalysts formed at different pyrolysis temperatures, (d) in different bases and (e) in different solvents. Reaction conditions: morpholine (1.0 mmol), paraformaldehyde (1.5 mmol), catalyst (20 mg), NaOH (0.2 mmol), O_2 (0.5 MPa), CH_3CN (2 mL), 60 °C, 12 h. Yields were determined using GC with *n*-dodecane as a standard.

dimorpholinomethane can be generated *via* condensation of **1a** with paraformaldehyde without a nano-Au catalyst.[29] *N*-Methyl morpholine can be formed *via* the reductive amination of **1a** with paraformaldehyde in the presence of water over a catalyst.[29,60] 4-(Methoxymethyl)morpholine is the possible intermediate which was observed in our previous report.[29]

$CoCl_2$ and the complex of $CoCl_2$ coordinated with 1,10-phenanthroline (1,10-Ph) show no activity for the reaction. CoNC-700-WA was synthesized *via* the same method without acid etching, however it showed negligible catalytic activity for the reaction (Fig. 1b). After acid etching, an excellent yield of **1b** was obtained over CoNC-700, which indicated that metallic cobalt and cobalt oxide were not the active metal species. CoNC-700-NP was prepared *via* impregnation of $CoCl_2$ on an XC-72R support and subsequence reduction with $NaBH_4$, but **1b** was not obtained under the same reaction conditions. The above results indicated that nano metallic cobalt and cobalt oxide were not the active metal species. CoNC-700-$CoBr_2$ was synthesized *via* the same method using $CoBr_2$ and 1,10-Ph as precursors, and the yield of **1b** was 59%, suggesting that the anion of the cobalt salt plays an important role for the formation of the active CoNC catalyst. CoNC-700-ZIF-8 was synthesized *via* pyrolysis of the $CoCl_2$-based ZIF-8, and the yield of **1b** was 51%. This suggests that the unique structure of the CoNC-700 was the source of the activity for the carbonylation reaction.

According to previous reports, the pyrolysis temperature affects the electronic structure of MNC catalysts.[61] Next, CoNC catalysts pyrolyzed at different temperatures (500, 600, 700, 800, 900, and 1000 °C) were synthesized to study the effects of the CoNC structure on the reaction. The yield of **1b** was 24% when CoNC was pyrolyzed at 500 °C. Upon increasing the pyrolysis temperature, the yields of **1b** were increased. The highest yield of **1b** was obtained over CoNC-700. Increasing the pyrolysis temperature further resulted in a decrease in the yields of **1b**, and the yield of **1b** decreased to 20% over CoNC-1000 (Fig. 1c). The BET surface area of the CoNC catalysts at different pyrolysis temperatures was tested. The BET surface areas of CoNC-600, CoNC-700 and CoNC-800 were found to be 321, 528, and 345 $m^2\ g^{-1}$ respectively, which suggests that a higher surface area is advantageous for the reaction (Table S2, ESI†). According to the XRD spectra, CoNC-700 shows the best dispersion, which is a possible reason for its high activity (Fig. 2a).

In the absence of a base additive, the yield of **1b** was obviously decreased, which suggests that a base is necessary for the reaction to proceed (Fig. 1d). The yield of **1b** was increased to 55% from 27% when 0.2 equiv. of KOH was added, probably because the base favors the depolymerization of paraformaldehyde. Na_2CO_3 and NaOH obviously improved the reaction outcome, and the highest yield of **1b** was obtained when 0.2 equiv. of NaOH was added. The organic base *t*BuONa was tested, but it did not promote the reaction as well as the inorganic bases did, possibly because the organic base was unstable under the reaction conditions. The effect of the NaOH

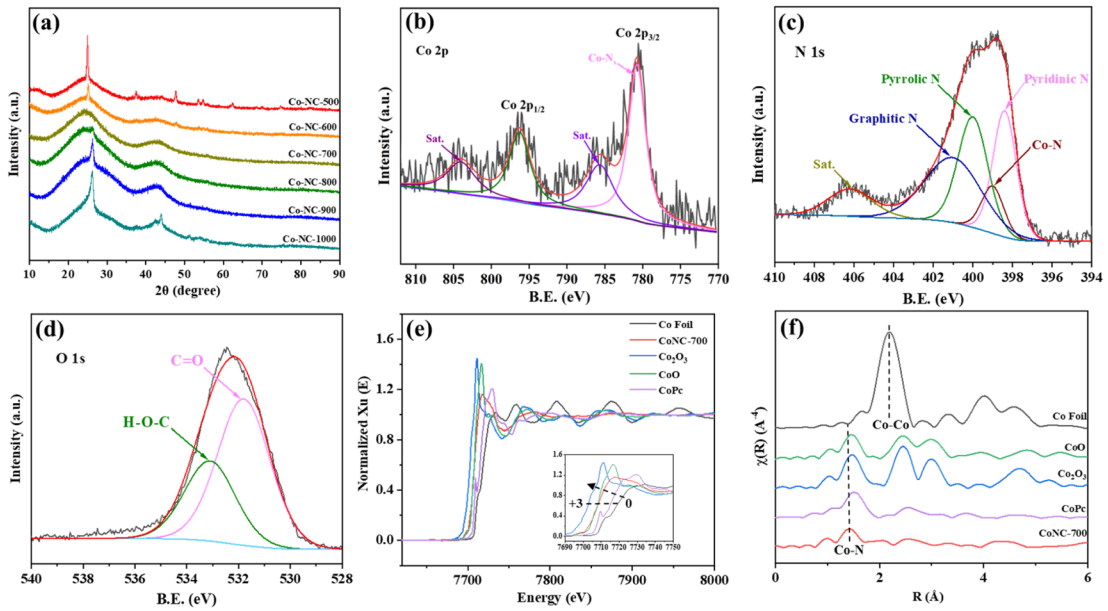

Fig. 2 (a) XRD patterns of CoNC pyrolyzed at different temperatures. High resolution XPS spectra of CoNC-700: (b) Co 2p region; (c) N 1s region; and (d) O 1s region. (e) Co K-edge XAFS spectra. (f) Fourier-transform k^3-weighted R space χ XAFS spectra of CoCN-700 with comparison to standard Co foil, CoO, Co_2O_3 and CoPc.

loading on the reaction was studied, and it was found that the yield of **1b** decreased as the NaOH loading decreased.

CoNC-700 showed low activity in weak polarity *n*-heptane solvent, and the yield of **1b** was only 41% (Fig. 1e). The yields of **1b** were 35% and 34% in tetrahydrofuran (THF) and 1,4-dioxane, respectively, which suggests that an obvious solvent effect exists. The yield of **1b** was obviously increased in γ-valerolactone, and the yield of **1b** was 77%. According to previous reports, acetonitrile (CH_3CN) is an excellent solvent for oxidation reactions.[62] Consistent with reported results, CH_3CN was the most effective solvent for the reaction, and the yield of **1b** was increased up to 90%. The strong polar solvent *N*,*N*-dimethylformamide (DMF) was not suitable for the reaction, and the yield of **1b** was only 23%. The effect of the oxygen pressure on the reaction was also investigated, and it was found that the yield of **1b** was decreased to 50% when the oxygen pressure was decreased to 0.1 MPa.

The stability of the CoNC-700 catalyst was investigated. After the reaction, the reaction solution was analyzed using ICP-MS after removal of the CoNC-700 catalyst *via* centrifugation (13 000 rpm). Only 0.0094 ppm cobalt was detected, which suggests that only a negligible quantity of cobalt from CoNC-700 was leached to the reaction solution. A hot filtration experiment was performed under the reaction conditions. After 6 h, the CoNC-700 catalyst was removed from the reaction system *via* hot filtration, the yield of **1b** was 43%. Subsequently, the autoclave was sealed and charged with 0.5 MPa O_2 and the reaction was continued for another 6 h, and the yield of **1b** was not significantly changed at 40%. This suggests that none of the active catalytic species was present in the reaction solvent.

CoNC-700 was applied to oxidative carbonylation of various amines with paraformaldehyde, and the results are shown in Table 1. N-Heterocycles are an important active chemical in pharmaceutical synthesis. The CoNC-700 catalyst was effective for the oxidative carbonylation of N-heterocycles including morpholine, piperidine and *N*-methyl piperazine with paraformaldehyde, and 67–90% of the target products were obtained (Table 1, entries 1–3). Primary aliphatic amines were obtained *via* the reductive amination of ammonia with aliphatic aldehydes, which in turn were sourced from the hydroformylation of olefines.[6] A 60% yield of *N*-octyl formamide was obtained *via* the reaction of *n*-octylamine with paraformaldehyde over CoNC-700 (Table 1, entry 4). The yield of *N*-hexyl-*N*-methyl formamide was 83% (Table 1, entry 5). Other secondary aliphatic amines such as *N*,*N*-dipropyl amine, *N*,*N*-dibutyl amine, and *N*,*N*-dihexyl amine showed excellent activity under the reaction conditions, and 68–79% target products yields were obtained, suggesting that secondary aliphatic amines showed better activity than primary aliphatic amines (Table 1, entries 6–8).

The oxidative carbonylation of aniline proceeded smoothly, and 72% yield of *N*-formyl aniline was obtained (Table 1, entry 9). Next, the effect of the functional groups on the aniline benzene ring was investigated. An aniline with an electron-donating methyl group showed excellent activity, and 85% yield of 4-methyl *N*-formyl aniline was obtained (Table 1, entry 10). This suggests that the electron-donating methyl substituent was favoured by the reaction. Halogen-substituted anilines were tested and 4-fluoro aniline, and 4-chloro aniline were also found to be suitable for the reaction, but slightly decreased yields of the target products obtained (Table 1, entries 11 and 12). This indicates that a halogen substituent on the benzene ring of the aniline is unfavoured by the reaction, and the negative effect increased with an increase of the atomic radius of the halogen

Table 1 Oxidative carbonylation of amines with paraformaldehyde[a]

Entry	Substrates	Products	Yield (%)
1		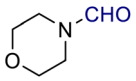	90
2		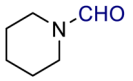	67[b]
3	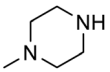	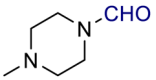	74[b]
4	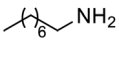	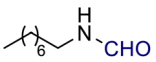	60[b]
5	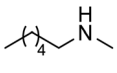	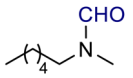	83[c]
6	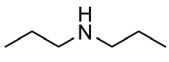	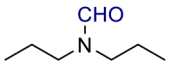	78[c]
7	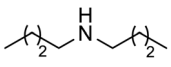	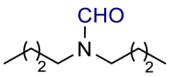	68[c]
8	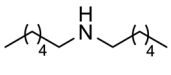	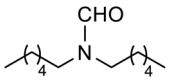	79[c]
9	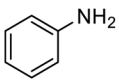	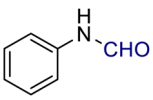	72[b]
10	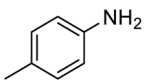	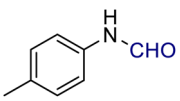	85[b]
11	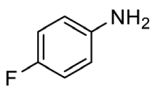	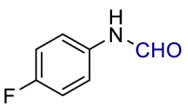	74[b]
12	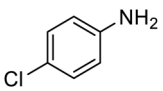	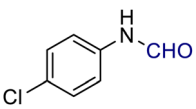	66[b]
13	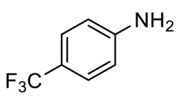	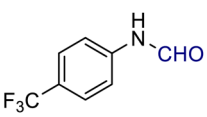	50[c]
14	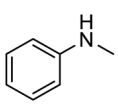	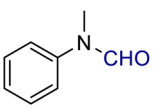	50[c]

[a] Reaction conditions: amine (0.5 mmol), paraformaldehyde (0.75 mmol), CoNC-700 (10 mg), NaOH (0.2 equiv.), O_2 (0.5 MPa), CH_3CN (2 mL), 60 °C, 12 h, isolated yields. [b] 120 °C, 24 h. [c] 140 °C, 12 h.

atoms. An aniline derivative possessing a strong electron-withdrawing trifluoromethyl group, could also be oxidatively carbonylated, and the yield of 4-trifluoromethyl formyl aniline was 50% (Table 1, entry 13). A secondary aromatic amine, *N*-methylaniline, was reacted over CoNC-700, and 50% yield of the *N*-formylated product was obtained (Table 1, entry 14).

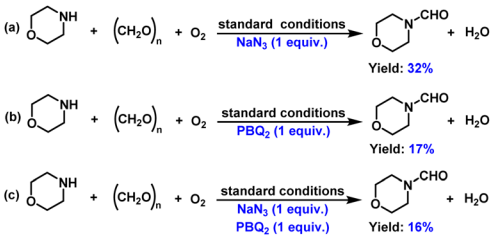

Scheme 2 Control experiments. The yields of the products were determined using GC-FID with dodecane as a standard. Standard conditions: **1a** (0.5 mmol), paraformaldehyde (0.75 mmol), CoNC-700 (10 mg), NaOH (0.2 equiv.), O_2 (0.5 MPa), CH_3CN (2 mL), 140 °C, 12 h.

To investigate the mechanism of the oxidative reaction, a series of control experiments were performed (Scheme 2). The yield of **1b** decreased to 32% from 90% in the presence of 1.0 equiv. of NaN_3, which suggests that singlet oxygen ($^1O_2$) is the active oxygen species. When *p*-benzoquinone (PBQ_2) was added, only 17% **1b** was obtained, indicating that superoxide anion (O_2^-) was also an active oxygen species. The yield of **1b** was 16% in the presence of PBQ_2 and NaN_3, further indicating that $^1O_2$ and O_2^- were the active oxygen species.

To reveal the relationship between the activity and structure of the catalyst, the prepared catalysts were characterized. As depicted in Fig. 2a, the XRD pattern of CoNC-700 showed only characteristic carbon peaks and no diffraction peaks in relation to Co species, indicating that the Co atoms were highly dispersed on the N-doped carbon. However, obvious diffraction peaks were observed when CoNC was formed by pyrolysis at other temperatures, which suggests that amorphous carbon is beneficial for the reaction. According to the above analysis (Fig. 1a), the cobalt was the active material of this CoNC catalyst. The BET surface area of the CoNC-700 catalyst was 528 $m^2\ g^{-1}$, which is beneficial for the formation of highly dispersed cobalt active sites.[63] N_2 adsorption–desorption isotherms exhibited typical type IV curves, along with an H1 hysteresis loop, suggesting the formation of a mesoporous structure which is favourable for the diffusion of reactants and products (Fig. S2, ESI†).

ICP-AES showed that the Co metal content in CoNC-700 was 2.45 wt%. X-ray photoelectron spectroscopy (XPS) was carried out to determine the surface electronic information relating to CoNC-700 (Fig. 2b–d and S3, S4, ESI†). The surface concentration of cobalt determined by XPS is 0.81 at%, which is negligibly higher than the ICP-AES result. This indicated that the cobalt was uniformly distributed on surface and in the body of CoNC-700. The characteristic peak of the Co $2p_{3/2}$ spectrum of CoNC-700 was mainly located at 780.78 eV, suggesting the presence of Co-N_x species (Fig. 2b).[64,65] The N 1s spectrum displays the presence of four nitrogen species, pyridinic-N (398.4 eV), Co-N_x (399.0 eV), pyrrolic-N (400.0 eV), and graphitic-N (401.0 eV) (Fig. 2c).[66,67] Two peaks at 531.84 and 533.14 eV were observed in the O 1s spectrum (Fig. 2d), which suggests that C=O and H–O–C species exist on the surface of CoNC-700.[68,69]

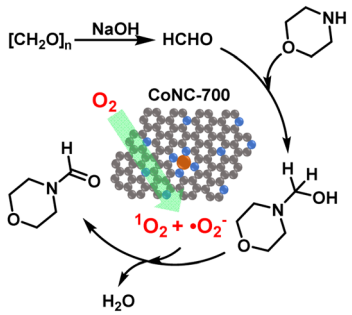

Fig. 3 The possible reaction mechanism of the oxidative carbonylation of **1a** with paraformaldehyde over the CoNC-700 catalyst.

To further identify the structure of the CoNC-700 catalyst, X-ray absorption fine structure (XAFS) spectroscopy was performed. The energy of the absorption edge of CoNC-700 was between cobalt phthalocyanin (CoPc) and CoO (Fig. 2e), indicating that the chemical state of the Co species was +2. From the Fourier-transform (FT) EXAFS analysis of CoNC-700, the first shell exhibits an obvious FT peak at 1.42 Å attributed to the CoN_x coordination.[66] Only this single peak appears in each FT-EXAFS spectrum of CoNC-700, which means that only Co single atom species are present in CoNC-700 (Fig. 2f). Therefore, CoN_x single atom sites are the possible catalytic active sites of the CoNC-700 catalyst.

A possible reaction mechanism of this CoNC-700-catalyzed oxidative carbonylation of **1a** with paraformaldehyde is proposed (Fig. 3). Firstly, paraformaldehyde was dissociated to formaldehyde in the presence of NaOH. Subsequently, molecular oxygen was converted to the active $^1O_2$ and O_2^- oxygen species over the CoNC-700 catalyst. At the same time, morpholino methanol was formed *via* coupling of **1a** with formaldehyde. Finally, the morpholino methanol was oxidatively dehydrogenated to **1b** by the active $^1O_2$ and O_2^- oxygen species over the CoNC-700 catalyst.

Conclusions

In conclusion, the oxidative carbonylation of a series of amines with paraformaldehyde was achieved on a non-noble metal CoNC-700 catalyst under mild conditions. Oxidative carbonylation of different amines, including heterocyclic amines, aliphatic primary amines, aliphatic secondary amines, aromatic primary amines and aromatic secondary amines with paraformaldehyde were realized over the CoNC-700 catalyst, and the corresponding *N*-formamides were obtained in moderate to good yields. A mechanistic investigation suggests that both singlet oxygen ($^1O_2$) and superoxide anions (O_2^-) are the active oxygen species of the oxidative carbonylation reaction. CoN_x single atom sites are the possible catalytic active sites on the CoNC-700 catalyst.

Data availability

The data and software from this article have been included as part of the ESI.†

Conflicts of interest

There are no conflicts to declare.

Acknowledgements

This work was financially supported by the China Postdoctoral Science Foundation (BX20190020 and 2019M660360), the High-level Talents launching Project of Shihezi University (RCZK202326), the PhD Talents launching Project of the First Affiliated Hospital of Shihezi University (BS202210), and the Tianchi Talent Project. We thank the Anhui Absorption Spectroscopy Analysis Instrument Co, Ltd for the XAFS measurements.

References

1 X. F. Wu, X. J. Fang, L. P. Wu, R. Jackstell, H. Neumann and M. Beller, *Acc. Chem. Res.*, 2014, **47**, 1041–1053.
2 J. B. Peng, F. P. Wu and X. F. Wu, *Chem. Rev.*, 2019, **119**, 2090–2127.
3 W. S. Putro, S. Ijima, S. Matsumoto, S. Hamura, M. Yabushita, K. Tomishige, N. Fukaya and J.-C. Choi, *RSC Sustain.*, 2024, **2**, 1613–1620.
4 I. T. Horvath and J. Rabai, *Science*, 1994, **266**, 72–75.
5 R. Franke, D. Selent and A. Börner, *Chem. Rev.*, 2012, **112**, 5675–5732.
6 D. M. Hood, R. A. Johnson, A. E. Carpenter, J. M. Younker, D. J. Vinyard and G. G. Stanley, *Science*, 2020, **367**, 542–550.
7 T. C. Jankins, W. C. Bell, Y. Zhang, Z.-Y. Qin, J. S. Chen, M. Gembicky, P. Liu and K. M. Engle, *Nat. Chem.*, 2022, **14**, 632–641.
8 Y. Nakagawa, M. Yabushita and K. Tomishige, *RSC Sustain.*, 2023, **1**, 814–837.
9 J. R. Martinelli, T. P. Clark, D. A. Watson, R. H. Munday and S. L. Buchwald, *Angew. Chem., Int. Ed.*, 2007, **46**, 8460–8463.
10 T. Xu, F. Sha and H. Alper, *J. Am. Chem. Soc.*, 2016, **138**, 6629–6635.
11 L.-C. Wang, B. Chen and X.-F. Wu, *Angew. Chem., Int. Ed.*, 2022, **61**, e202203797.
12 A. Kampwerth, T. B. Riemer, J. Pöttker-Menke, N. Oppenberg, A. M. Windisch, D. Vogt and T. Seidensticker, *RSC Sustain.*, 2024, **2**, 1797–1808.
13 V. R. Pattabiraman and J. W. Bode, *Nature*, 2011, **480**, 471–479.
14 B. Mahjour, Y. Shen, W. Liu and T. Cernak, *Nature*, 2020, **580**, 71–87.
15 A. R. Shelte, R. D. Patil and S. Pratihar, *RSC Sustain.*, 2024, **2**, 2615–2625.
16 C. L. Allen and J. M. J. Williams, *Chem. Soc. Rev.*, 2011, **40**, 3405–3415.
17 L. A. Shastri, S. L. Shastri, C. D. Bathula, M. Basanagouda and M. V. Kulkarni, *Synth. Commun.*, 2011, **41**, 476–484.
18 C. J. Gerack and L. McElwee-White, *Molecules*, 2014, **19**, 7689–7713.
19 P. Anastas and N. Eghbali, *Chem. Soc. Rev.*, 2010, **39**, 301–312.

20 F. Wang, J. D. Harindintwali, Z. Yuan, M. Wang, F. Wang, S. Li, Z. Yin, L. Huang, Y. Fu, L. Li, S. X. Chang, L. Zhang, J. Rinklebe, Z. Yuan, Q. Zhu, L. Xiang, D. C. W. Tsang, L. Xu, X. Jiang, J. Liu, N. Wei, M. Kästner, Y. Zou, Y. S. Ok, J. Shen, D. Peng, W. Zhang, D. Barceló, Y. Zhou, Z. Bai, B. Li, B. Zhang, K. Wei, H. Cao, Z. Tan, L.-b. Zhao, X. He, J. Zheng, N. Bolan, X. Liu, C. Huang, S. Dietmann, M. Luo, N. Sun, J. Gong, Y. Gong, F. Brahushi, T. Zhang, C. Xiao, X. Li, W. Chen, N. Jiao, J. Lehmann, Y.-G. Zhu, H. Jin, A. Schäffer, J. M. Tiedje and J. M. Chen, *Innovation*, 2021, **2**, 100180–100203.
21 S. M. Kernaghan, T. Coady, M. Kinsella and C. M. Lennon, *RSC Sustain.*, 2024, **2**, 578–607.
22 S. Tanaka, T. Minato, E. Ito, M. Hara, Y. Kim, Y. Yamamoto and N. Asao, *Chem.–Eur. J.*, 2013, **19**, 11832–11836.
23 M. C. Pichardo, G. Tavakoli, J. E. Armstrong, T. Wilczek, B. E. Thomas and M. H. G. Prechtl, *ChemSusChem*, 2020, **13**, 882–887.
24 Y. Zhang, X. Dai, J. Wang, J. Liang, J. Rabeah, X. Tian, X. Yao, Y. Wang and S. Pang, *ChemSusChem*, 2023, **16**, e202202104.
25 P. Preedasuriyachai, H. Kitahara, W. Chavasiri and H. Sakurai, *Chem. Lett.*, 2010, **39**, 1174–1176.
26 O. Saidi, M. J. Bamford, A. J. Blacker, J. Lynch, S. P. Marsden, P. Plucinski, R. J. Watson and J. M. J. Williams, *Tetrahedron Lett.*, 2010, **51**, 5804–5806.
27 L. Zhou, C. G. Freyschlag, B. Xu, C. M. Friend and R. J. Madix, *Chem. Commun.*, 2010, **46**, 704–706.
28 N. Shah, E. Gravel, D. V. Jawale, E. Doris and I. N. N. Namboothiri, *ChemCatChem*, 2014, **6**, 2201–2205.
29 Z. Ke, Y. Zhang, X. Cui and F. Shi, *Green Chem.*, 2016, **18**, 808–816.
30 I. Metaxas, E. Vasilikogiannaki and M. Stratakis, *Nanomaterials*, 2017, **7**, 440–450.
31 S. Kazemi, A. Mobinikhaledi and M. Zendehdel, *Chin. Chem. Lett.*, 2017, **28**, 1767–1772.
32 L. Zhang, Z. Han, X. Zhao, Z. Wang and K. Ding, *Angew. Chem., Int. Ed.*, 2015, **54**, 6186–6189.
33 Z. Ke, Z. Yang, Z. Liu, B. Yu, Y. Zhao, S. Guo, Y. Wu and Z. Liu, *Organ. Lett.*, 2018, **20**, 6622–6626.
34 Y. Shen, Q. Zheng, Z.-N. Chen, D. Wen, J. H. Clark, X. Xu and T. Tu, *Angew. Chem., Int. Ed.*, 2021, **60**, 4125–4132.
35 D. Cheng, M. Wang, L. Tang, Z. Gao, X. Qin, Y. Gao, D. Xiao, W. Zhou and D. Ma, *Angew. Chem., Int. Ed.*, 2022, **61**, e202202654.
36 X. Dai, T. Li, B. Wang, C. Kreyenschulte, S. Bartling, S. Liu, D. He, H. Yuan, A. Brückner, F. Shi, J. Rabeah and X. Cui, *Angew. Chem., Int. Ed.*, 2023, **62**, e202217380.
37 A. Rodil, I. von Ossowski, M. Nyyssönen, Y. Tian, M. Hallamaa, J. Deska, M. Bomberg and S. Scheller, *RSC Sustain.*, 2024, **2**, 3264–3275.
38 M. Nasrollahzadeh, N. Motahharifar, M. Sajjadi, A. M. Aghbolagh, M. Shokouhimehr and R. S. Varma, *Green Chem.*, 2019, **21**, 5144–5167.
39 A. Corma, S. Iborra and A. Velty, *Chem. Rev.*, 2007, **107**, 2411–2502.
40 T. Sakakura, J.-C. Choi and H. Yasuda, *Chem. Rev.*, 2007, **107**, 2365–2387.
41 A. Goeppert, M. Czaun, J.-P. Jones, G. K. S. Prakash and G. A. Olah, *Chem. Soc. Rev.*, 2014, **43**, 7995–8048.
42 M. Qian, M. A. Liauw and G. Emig, *Appl. Catal., A*, 2003, **238**, 211–222.
43 J. Bin Yeo, J. Ho Jang, Y. In Jo, J. Woo Koo and K. Tae Nam, *Angew. Chem., Int. Ed.*, 2024, **63**, e202316020.
44 J. B. Zimmerman, P. T. Anastas, H. C. Erythropel and W. Leitner, *Science*, 2020, **367**, 397–400.
45 U. Martinez, S. Komini Babu, E. F. Holby, H. T. Chung, X. Yin and P. Zelenay, *Adv. Mater.*, 2019, **31**, 1806545.
46 Y. He, S. Liu, C. Priest, Q. Shi and G. Wu, *Chem. Soc. Rev.*, 2020, **49**, 3484–3524.
47 X. Lei, Q. Tang, Y. Zheng, P. Kidkhunthod, X. Zhou, B. Ji and Y. Tang, *Nat. Sustain.*, 2023, **6**, 816–826.
48 W. Mo, X. Tan and L. Zhao, *RSC Sustain.*, 2024, **2**, 2709–2716.
49 T. Senthamarai, V. G. Chandrashekhar, N. Rockstroh, J. Rabeah, S. Bartling, R. V. Jagadeesh and M. Beller, *Chem*, 2022, **8**, 508–531.
50 B. Li, J. Kou, G. Zeng, J. Ma and Z. Dong, *Acc. Chem. Res.*, 2023, **13**, 16286–16299.
51 R. V. Jagadeesh, H. Junge, M.-M. Pohl, J. Radnik, A. Brückner and M. Beller, *J. Am. Chem. Soc.*, 2013, **135**, 10776–10782.
52 X. Cui, Y. Li, S. Bachmann, M. Scalone, A.-E. Surkus, K. Junge, C. Topf and M. Beller, *J. Am. Chem. Soc.*, 2015, **137**, 10652–10658.
53 A. V. Iosub and S. S. Stahl, *Organ. Lett.*, 2015, **17**, 4404–4407.
54 K. Sun, H. Shan, R. Ma, P. Wang, H. Neumann, G.-P. Lu and M. Beller, *Chem. Sci.*, 2022, **13**, 6865–6872.
55 W. Ai, R. Zhong, X. Liu and Q. Liu, *Chem. Rev.*, 2019, **119**, 2876–2953.
56 S. Shang, L. Wang, W. Dai, B. Chen, Y. Lv and S. Gao, *Catal. Sci. Technol.*, 2016, **6**, 5746–5753.
57 K.-k. Sun, J.-l. Sun, G.-P. Lu and C. Cai, *Green Chem.*, 2019, **21**, 4334–4340.
58 T. Senthamarai, V. G. Chandrashekhar, N. Rockstroh, J. Rabeah, S. Bartling, R. V. Jagadeesh and M. Beller, *Chem*, 2022, **8**, 508–531.
59 W. Wang, L. Ma, X. Jiang, H. Wang, Z.-H. He, K. Wang, Y. Yang and Z.-T. Liu, *ACS Sustainable Chem. Eng.*, 2022, **10**, 14636–14647.
60 Z. Ke, X. Cui and F. Shi, *ACS Sustainable Chem. Eng.*, 2016, **4**, 3921–3926.
61 S. Ji, Y. Chen, X. Wang, Z. Zhang, D. Wang and Y. Li, *Chem. Rev.*, 2020, **120**, 11900–11955.
62 M. Hua, J. Song, X. Huang, H. Liu, H. Fan, W. Wang, Z. He, Z. Liu and B. Han, *Angew. Chem., Int. Ed.*, 2021, **60**, 21479–21485.
63 X. Liang, N. Fu, S. Yao, Z. Li and Y. Li, *J. Am. Chem. Soc.*, 2022, **144**, 18155–18174.
64 T. Su, K. Sun, G. Lu and C. Cai, *ACS Sustainable Chem. Eng.*, 2022, **10**, 3872–3881.
65 J. Xie, B.-Q. Li, H.-J. Peng, Y.-W. Song, J.-X. Li, Z.-W. Zhang and Q. Zhang, *Angew. Chem., Int. Ed.*, 2019, **58**, 4963–4967.
66 Y. Pan, R. Lin, Y. Chen, S. Liu, W. Zhu, X. Cao, W. Chen, K. Wu, W.-C. Cheong, Y. Wang, L. Zheng, J. Luo, Y. Lin,

Y. Liu, C. Liu, J. Li, Q. Lu, X. Chen, D. Wang, Q. Peng, C. Chen and Y. Li, *J. Am. Chem. Soc.*, 2018, **140**, 4218–4221.
67 X. Li, A.-E. Surkus, J. Rabeah, M. Anwar, S. Dastigir, H. Junge, A. Brückner and M. Beller, *Angew. Chem., Int. Ed.*, 2020, **59**, 15849–15854.
68 C. Liu, T. Li, X. Dai, J. Zhao, D. He, G. Li, B. Wang and X. Cui, *J. Am. Chem. Soc.*, 2022, **144**, 4913–4924.
69 L. Zhang, T. Li, X. Dai, J. Zhao, C. Liu, D. He, K. Zhao, P. Zhao and X. Cui, *Angew. Chem., Int. Ed.*, 2023, **62**, e202313343.